Journal of Environmental Chemical Engineering 13 (2025) 115226

Contents lists available at ScienceDirect

Journal of Environmental Chemical Engineering

journal homepage: www.elsevier.com/locate/jece

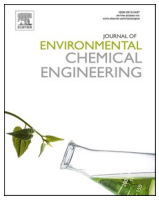

Continuous extraction of xylose to Dowtherm A via esterification with 1-napthalene boronic acid from bagasse acid hydrolysate

Peter J. van der Wal, Jean-Paul Lange, Sascha R.A. Kersten, M. Pilar Ruiz *

Sustainable Process Technology, Faculty of Science and Technology, University of Twente, Enschede 7522 NB, the Netherlands

ARTICLE INFO

Keywords:
Extraction
Xylose
Furfural
Boronate ester

ABSTRACT

Previous studies identified esterification with 1-napthalene boronic acid and subsequent extraction to Dowtherm A as a means of separating xylose from an aqueous stream. It was also shown that the xylose-boronate ester can be converted to furfural at high yields. To further investigate the possibilities of a large-scale continuous process for converting biomass (in this case sugarcane bagasse) to furfural, the reactive extraction is further studied in this work. A kinetic model for the extraction rate of xylose in both a batch and continuous system is made and verified using a model solution of xylose in water, the findings are also confirmed for actual biomass, and a multistage countercurrent mixer-settler cascade is modeled. This demonstrated the possibility of recovering more than 90 % of the xylose in a 50 g/L feed stream with 3 stages and a total residence time of 10 minutes.

1. Introduction

To reduce the consumption of fossil resources, biomass is a possible alternative. One possible route is to convert the hemicellulose fraction of biomass to furfural, promising sustainable platform chemical for the production of chemicals and fuels [1–3]. Furfural is made from the C5 sugars (pentoses) present in the hemicellulose fraction, usually by dehydration with sulfuric acid (acid hydrolysis). This, however, also produces by-products, such as C6 sugars, furanics and acetic acid. Furthermore, current state-of-the-art furfural production processes are 50 mol% selective for furfural from the pentosan fraction of biomass [2, 3]. More selectivity can be obtained by selectively extracting these sugars from the aqueous phase before converting them to furfural [4–6]

One possibility to separate the pentoses from the hydrolysate is by extracting them to an apolar organic phase. As sugars are very polar, some chemistry is needed for this extraction. Boronic acids can react with the -OH groups of sugars to form apolar boronate esters. This has been shown to work well for especially xylose, a mayor part of the C5 fraction of hemicellulose [7–9]. Furthermore, the esters formed can then be converted to furfural at higher yields compared to starting from xylose [5,6,10]

When investigating this extraction, it is key to place it in the broader context of a possible chemical process. Although extracting xylose selectively from an aqueous stream is useful in a number of applications, a particular application is that of furfural production. The added benefit here is that the sugar-boronate ester can be hydrolyzed in the same reactor as where the furfural is produced. An example process is shown in Fig. 1, derived from [10].

First, sugarcane bagasse is hydrolyzed around 120 °C in a 1 wt% H_2SO_4 solution to produce a solution of roughly 50 g/L sugars in water, with furfural, 5-HMF, acetic acid and humins (polymerized furfural/5-HMF) as contaminants [11,12]. The reactive extraction then selectively extracts out the xylose, which is converted to furfural in another reactor in an acidic aqueous medium. Most of the furfural partitions to the organic phase after the reaction if the aqueous phase contains salts, such as Na_2SO_4, allowing for full recovery furfural by only separating it from the organic phase [6,10]. If the organic phase has a boiling point above that of furfural, a simple distillation suffices.

A key part of this process that affect the design and operation of the reactive extraction is that both feed streams are above ambient temperature: the aqueous phase comes from hydrolysis at 120 °C, and the organic from furfural recovery by distillation above the boiling point of furfural (162 °C). It would therefore be beneficial if the extraction could be carried out at elevated temperatures, as it would reduce the amount of cooling required.

The bottoms fraction of the furfural distillation column is also recycled in the process, which is rich in NBA and Dowtherm A. Only furfural and any other lights are removed by means of distillation. This means that it is key to determine whether any heavy contaminants from the acid bagasse hydrolysate ABH migrate to the organic phase during

* Corresponding author.
E-mail address: m.p.ruizramiro@utwente.nl (M.P. Ruiz).

https://doi.org/10.1016/j.jece.2024.115226
Received 19 July 2024; Received in revised form 17 December 2024; Accepted 25 December 2024
Available online 25 December 2024

extraction, and whether further separation is needed.

Furthermore, after extraction, the raffinate stream is still rich in H_2SO_4. Due to its polar nature, it is unlikely that much is extracted to the organic phase. It is therefore worth to investigate whether the raffinate can be reused in the hydrolysis. For this, it should not lose much sulfuric acid or contain any contaminants which might accumulate in this recycled stream.

Previous research from our group [8] identified Dowtherm A as a suitable solvent for this extraction. High extractive yields and fast kinetics were demonstrated when combined with 1-napthalene boronic acid (NBA), as well as the high-yielding conversion to xylose. Since Dowtherm A has a boiling point above that of furfural, Dowtherm A and NBA are used as a solvent in this work. However, little has been done on developing the extraction with these chemicals to an actual process. The aim of this paper is to investigate this and develop and size a process for extracting xylose from a biomass hydrolysate stream.

To this end, a kinetic model of the extraction has been made, as the reactive extraction is not instantaneous. This model was made using new batch experiments with a model solution of only xylose in water, and then used to predict the behavior of a single-stage continuous system. The performance of the model in this case has also been experimentally verified. Furthermore, some extra batch experiments have been done with an acid hydrolysate of sugarcane bagasse. This is to not only verify that the findings with the model solution are applicable to a real system, but also to investigate whether the hydrolysate, once the sugars have been extracted, can be re-used in the hydrolysis. The final model was used to determine the dimensions of a continuous counter-current mixer-settler cascade for the extraction of xylose.

2. Materials and methods

2.1. Chemicals

The following chemicals were used: deionized water (Elix Essential 3, 14 MΩ•cm), Dowtherm A (Thermo Scientific), D-xylose (>99 %, Sigma Aldrich), 1-naphthalene boronic acid (NBA, >97 %, Boron Molecular) H_2SO_4 (96 %, Supelco), KOH (>90 %, Sigma Aldrich), NaOH (>97 %, Sigma Aldrich), Thymol Blue (Sigma Aldrich) L-arabinose (>99 %, Sigma Aldrich), D-glucose (>99 %, Sigma Aldrich), D-galactose (>99 %, Sigma Aldrich), furfural (99 %, Sigma Aldrich), 5-hydroxymethylfurfural (HMF, >99 %, Sigma Aldrich), Acetic acid (96 %, Supelco) and tetrahydrofuran (THF, LC grade, Supelco).

2.2. Kinetics and equilibria

For determining the kinetics and equilibria of the extraction and determining the solubility of NBA, a 250 mL jacketed glass vessel was used. This was connected to a Julabo F-32 circulating water for constant temperature. To measure the temperature inside the vessel, a K-type thermocouple was used. Stirring was accomplished with a mechanical overhead stirrer. The vessel was open to atmosphere via a 250 mm reflux condenser. Samples could be taken with a small Teflon tube fitted with a Luer-Lock connector. A photo of the apparatus is provided in S1.

For measuring the kinetics and equilibria of the extraction, the vessel was loaded with a 100 mL solution of 5 wt% xylose in water, 100 mL Dowtherm A and 11.5 g NBA. This corresponded to 2 moles NBA per mole xylose. The liquid contents were heated inside the vessel before the NBA was added. Once the NBA had been added, the vessel closed and the stirrer started, a timer was started to take samples on a regular interval. These samples would be taken via the aforementioned Teflon tube with a 10 mL syringe. The contents of the syringe were quickly transferred to a glass centrifuge vial, centrifuged at 3000 RPM to separate the organic and aqueous phases which were then transferred to separate syringes. From taking the sample to both phases being in separate syringes took less than three minutes. The centrifuge ran for one minute, mostly spinning up and down, and only operating at 3000 RPM for a few seconds. This was always enough to separate the sample into the separate phases (water, organic and any undissolved NBA).

The syringes containing the samples were not immediately analyzed. Instead, aqueous samples were placed in an ice bath for at least two

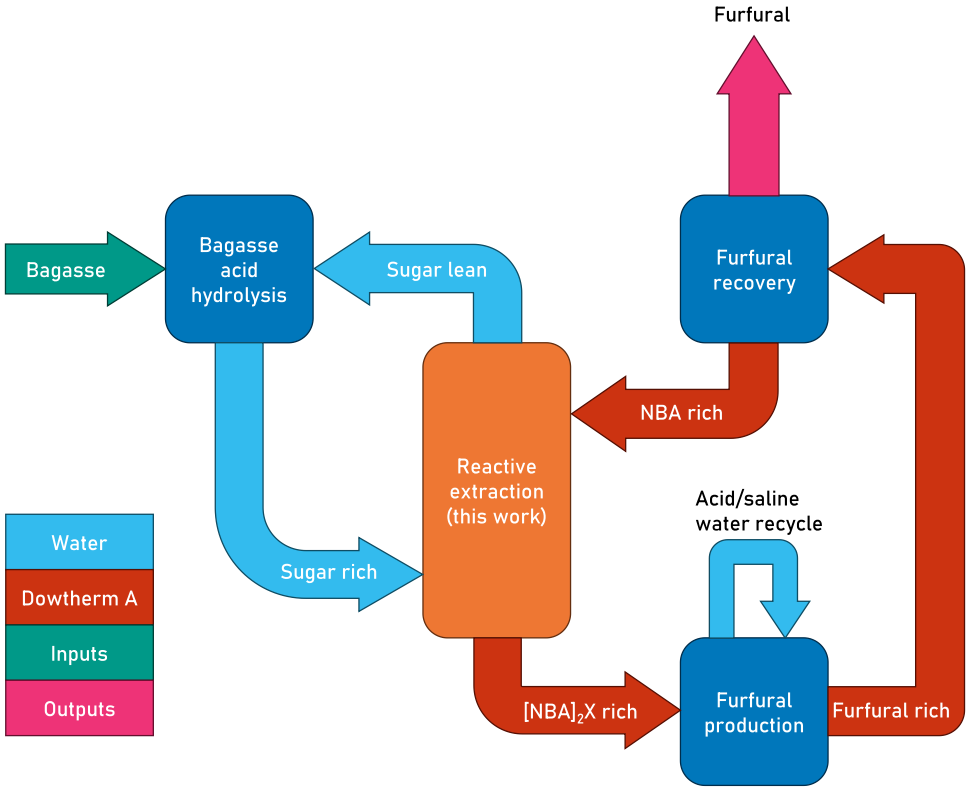

Fig. 1. Example process for converting biomass to furfural via a boronate ester intermediate.

hours. The sample was then filtered with a 0.20 μm regenerated cellulose filter and transferred to a 2 mL vial, ready for analysis. The ice bath ensure that any NBA would crystallize out prior to the filtration step and not in the 2 mL vial, as the analysis equipment used on the aqueous phase could not handle solids present in the sample. This procedure was not followed for the organic samples. Instead, they cooled down in ambient air for two hours before being filtered and transferred to 2 mL vials for analysis. Some samples did crystallize out this way in the vials, but this proved not to influence the analysis.

2.3. Solubility measurements

For measuring the solubility of NBA in water at various temperatures, the same 250 mL jacketed glass vessel was filled with 200 mL of water. Enough NBA was then added to ensure the solution would be saturated. For early measurements, this was confirmed by seeing solid NBA left at the end of the experiment. Later, as the solubility could be predicted to some degree, at least three times the amount of NBA needed to saturate the solution was added. The solution was heated to the desired temperature and stirred for at least 16 hours. Stirring would then be stopped, and 6 samples of 20 mL were taken through a 0.20 μm regenerated cellulose filter into a syringe. The syringes were allowed to cool down to ambient temperature, and the contents transferred to a petri dish. Some samples would crystallize out in the syringe, but these solids were transferred to the petri dish together with all the liquid. These dishes were first dried at 90 °C and later placed in a desiccator to cool down. Before any sample was added, the dry dishes were weighed. The syringes containing the sample were weighed before and after adding the sample to the dish, determining the amount of sample added to each dish. The dishes were then placed in an oven at 90 °C until all water had evaporated. This took a couple of hours each time, until it was visually confirmed that no water was left. After this, the dishes were cooled down in a desiccator and weighed. Knowing the amount of sample added to each dish, and the amount of solids left in the dish, the solubility of NBA in water could be determined over a range of temperatures. It should be noted that the solids present in the dishes after drying were analyzed by FTIR, which revealed that the remaining solid was not NBA, but the boroxine trimer $[NBA]_3$. As the molar mass is different from NBA to $[NBA]_3$, data processing took this into account.

2.4. Partitioning measurements

For measuring the partitioning of NBA between water and Dowtherm A, a Julabo SW23 shaking water bath was used. Five 150 mL jars were placed inside this bath and shaken at 200 RPM for at least 16 hours at the temperature the partition was to be determined. To each jar, 25 mL water and 25 mL Dowtherm A was added. The combination of a relatively large jar and a small amount of fluid ensured that the phases mixed well, as demonstrated by the content becoming a white emulsion in all experiments. Per jar, either 2, 4, 6, 8 or 10 mg of NBA was added. This amount was carefully chosen so that all the NBA could dissolve in the added water, guaranteeing that all NBA would dissolve and partition over both phases. After shaking for 16 hours, a sample was taken of the aqueous phase and filtered with a 0.20 μm regenerated cellulose filter to remove any Dowtherm A and foreign solids. The NBA concentration was then determined with UV–vis spectroscopy. By means of a mole balance the amount of NBA in the organic phase was determined, allowing for the partition coefficient to be determined.

2.5. Continuous extraction experiments

For continuous extraction experiments, a small glass jacketed reactor was used. The internal volume, taking into account the size of the internals, was determined to be 61 ± 2 mL. Through the jacket, hot water was pumped from a Julabo F32 circulating hot water bath through 10 mm PVC hoses with added external insulation. The temperature inside the reactor was measured with a K-type thermocouple. Stirring was accomplished by a mechanical stirrer, of which the power consumption was measured over time with a PicoLog ADC-24. The reactants entered the reactor through a hole in the side, and out via the top. A section of 30 cm PTFE tubing allowed for the samples to cool down before being captured in a glass centrifuge vial. The vials were put on ice and all centrifuged at once, after which xylose was quantified in the aqueous phase using HPLC, and $[NBA]_2X$ in the organic phase using FTIR.

The feed was pumped into the reactor using a Masterflex® L/S® peristaltic pump, using Masterflex® L/S® 14 platinum-cured silicone tubing (ID 1.6 mm) in Masterflex® L/S® Easy-Load® II pump heads. Two heads were attached to one pump body, simultaneously pumping the Dowtherm A and the aqueous xylose solution. Using a peristaltic pump allowed for the NBA to be pumped with the Dowtherm A as a slurry. The NBA did have to be sieved for the slurry to be pumpable: only when particles smaller than 500 μm were used, the silicone tubing through which the slurry flowed would not block. The xylose solution was fed to the pump from a 1 L vessel, which was kept at 80 °C during the experiment. The vessel was equipped with a trap to allow in air as the solution was pumped out but prevented excessive evaporation of the solution. The entire CSTR (continuously stirred tank reactor) setup is shown on a photo in S2.

2.6. Bagasse hydrolysis

Sugarcane Bagasse (*Saccharum officinarum*) was hydrolyzed to produce acid bagasse hydrolysate (ABH). This was made by adding 60 g of dry bagasse to 600 mL water with 6 mL H_2SO_4 and letting it react at 120 °C for four hours. All reagents were added at room temperature to a 1 L autoclave (Premex GmbH) and stirred by mechanical agitation. Heating was done with electric heaters in the reactor wall and lid, heating the reagents to 120 °C, as measured by a K-type thermocouple in a thermowell inside the reactor. The reactor was cooled by circulating tap water through the reactor wall, which started four hours after heating started. Afterwards, the product was vacuum filtered. The product volume was measured, and per 100 mL, 10 g of dry bagasse was added, and the exact same procedure in the 1 L autoclave was followed to produce the final ABH.

2.7. Analytical methods

Aqueous samples were analyzed by HPLC to quantify the xylose, glucose, arabinose, galactose, furfural, 5-HMF and acetic acid content. An Agilent 1200 series HPLC was used, either equipped with a Hi-Plex-H+ column at 65 °C with 5 mmol/L H_2SO_4 as an eluent for furfural, 5-HMF and acetic acid, or with a Hi-Plex-Pb column with water as eluent for all sugars. For detection, a refractive index and UV–vis detector were used. Samples on the H+ column were run as-is, while samples on the Pb column were neutralized first to a pH of 6–8 by adding solid KOH.

Organic samples were analyzed by FTIR to quantify the $[NBA]_2X$ content. The peak area at 1206 cm^{-1} was used for quantification, as it was shown to be unique for $[NBA]_2X$ in Dowtherm A. For FTIR measurements, a Bruker Tensor 27 FTIR was used, with a Pike MIRacle ATR attachment. Prior to ATR measurements, a background was recorded of the solvent used. This was subtracted from the sample spectrum.

NBA in water was quantified with UV–vis, using a Hach-Lange DR5000 with 10 mm quartz cuvettes. The peak area of the peak around 280 nm was used for quantification. Using the peak area, any aberrations in the baseline due to small, dissolved amounts of Dowtherm A in the sample could be compensated for.

Microcarbon residue tests (MCRT) were conducted according to ASTM-D4530 −15 using large 4-dram vials. Each sample was run in triplicate with 5 g per vial. Vials were dried in an oven prior to MCRT analysis at 105 °C.

GPC was used to qualify the weight distribution of aqueous and organic sample. All samples were diluted 20x in THF and handled by only glass equipment, to prevent any contamination from other polymers. An Agilent 1260 Infinity series chromatograph was used, with three GPC PLgel 3 m MIXED-E columns in series. THF was used as mobile phase at 1 mL/min, and the columns were heated to 40 °C. Calibration was done with polystyrene standards with molecular weights ranging from 0.162 to 27.81 kDa. For detection, a refractive index and UV detector were used, with the UV detector operating at 254 nm.

Differential scanning calorimetry and thermogravimetric analysis (TGA-DSC) were performed with a Netzsch STA449 F3. The following temperature profile was used:

- Isothermal 20 min at 35 °C,
- Dynamic 3 °C/min to 300 °C,
- Isothermal 30 min at 300 °C,
- Dynamic 3 °C/min to 35 °C,
- Isothermal 30 min at 35 °C

The analysis was carried out under 100 mL/min N_2 gas, with sample of 8.8910 mg NBA.

All samples were filtered prior to analysis with a 0.20 μm regenerated cellulose filter.

2.8. Statistical methods

In all graphs in this work, all error bars denote a 95 % analytical confidence interval determined by the calibration curves used for each instrument, unless denoted otherwise. All calibration curves can be found in the supporting information (S2–4).

For fitting either the Van 't Hoff or Arrhenius equation to any data, the following equations were used:

$$\log(k) = A + B\frac{T - T_{ref}}{T} \text{ where } A = \ln(k_0) - \frac{E_{act}}{RT_{ref}} \text{ and } B = \frac{E_{act}}{RT_{ref}} \quad (1)$$

$$\log(K) = A + B\frac{T - T_{ref}}{T} \text{ where } A = \frac{\Delta S_0}{R} - \frac{\Delta H_0}{RT_{ref}} \text{ and } B = \frac{\Delta H_0}{RT_{ref}} \quad (2)$$

These were modified from the original by introducing a reference temperature T_{ref}. This was always chosen to be the mean of the temperatures in the dataset to which either k or K is fitted. The reference temperature is then used to make the original temperature dimensionless and centered around 0 by transforming it to (T-T_{ref})/T. This transformation makes the resulting fit more accurate, i.e., the prediction interval of either k or K for a certain temperature becomes smaller [13].

For predicting the solubility, the following correlation was used [14]:

$$\log(x) = \frac{\Delta H_m}{R}\left(\frac{1}{T_m} - \frac{1}{T}\right) \quad (3)$$

Herein, x denotes the mole fraction of solute at equilibrium, R the universal gas constant, ΔH_m the heat of melting and T_m the melting temperature of the solute. For fitting, this correlation was modified much like the Arrhenius and Van 't Hoff Equations:

$$\log(x) = A + B\frac{T - T_{ref}}{T} \text{ where } A = \frac{\Delta H_m}{R}\left(\frac{1}{T_m} - \frac{1}{T_{ref}}\right) \text{ and } B = \frac{\Delta H_m}{RT_{ref}} \quad (4)$$

For all fits of either k, K or solubility, the fit was made using this aforementioned dimensionless temperature and the natural logarithm of the data, yielding a fit of the form A+B*x. All datapoints were weighed by the inverse relative size of their 95 % confidence interval of the logarithm of the data (W):

$$W = \frac{\log(x)}{\log\left(\frac{x+\Delta x}{x}\right)} \quad (5)$$

Here, x denotes a measured variable, and Δx the size of the 95 % confidence interval. This weighing produced fits with the smallest prediction interval, as datapoints with larger errors relative to the measured value weigh less, while taking into account that the logarithm of the data is used for fitting. All weights were normalized, i.e., spanning from 0 to 1.

To fit a kinetic rate constant k to a list of concentrations over time, it is customary to construct a model that predicts concentration over time for a certain rate constant k. To obtain the actual value of k, the model would be run for several values of k, until the least-squares fit of the data to the model has been found. This was also attempted in this work, and produced a satisfactory value of k_{1e}. The model used is described in Eqs. (32)–(34).

2.9. NBA concentration balance

As stated previously, NBA could not be determined by the analytical methods available. To determine the concentration for any amount of NBA at any temperature in any combination of water and Dowtherm A, a balance was made. In this balance, all NBA that is present (either by adding it to the reaction mixture or released by hydrolysis of $[NBA]_2X$) is in one of three states: as a solid, or dissolved in either water or Dowtherm A. The goal of the balance is to determine how much NBA is in each state for a given amount of NBA, organic and aqueous volume and temperature.

The sum of NBA in these three states has to be equal to the total amount present in the system:

$$n_{NBA} = n^s_{NBA} + n^{aq}_{NBA} + n^{org}_{NBA} \quad (6)$$

Here, n denotes the amount of moles, and the superscripts s, aq and org in which state the NBA is: solid, or dissolved in water or Dowtherm A respectively. For the dissolved NBA, it is easier to work with concentrations c in a volume V:

$$n_{NBA} = n^s_{NBA} + c^{aq}_{NBA}V^{aq} + c^{org}_{NBA}V^{org} \quad (7)$$

Knowing the partitioning of NBA over water and Dowtherm A at a certain temperature, this can be written with only one concentration and the partition coefficient K_4 as a function of temperature:

$$n_{NBA} = n^s_{NBA} + c^{aq}_{NBA}(V^{aq} + K_4(T)V^{org}) \quad (8)$$

This leaves two unknows: the amount of solid NBA and the concentration in the aqueous phase. To determine this, one can discern two cases which gives the solution for one of the unknowns:

1. The total amount of NBA is small and all of it is dissolved, i.e. $n^s_{NBA} = 0$
2. The total amount of NBA is large, and the aqueous and organic phase are saturated and solid NBA is present; i.e. $c^{aq}_{NBA} = c^{aq,sat}_{NBA}(T)$

To determine in which of the two cases the system is, the total amount of moles that can be dissolved in the saturated system need to be determined (n^{sat}_{NBA}):

$$n^{sat}_{NBA}(T) = c^{aq,sat}_{NBA}(T)(V^{aq} + K_4(T)V^{org}) \quad (9)$$

If the total amount of moles is lower than this amount, the system is in case 1. Otherwise, it is in case 2.

This method allows for the determination of the NBA concentration for any temperature, amount of total NBA and volume of aqueous and organic phase. It can also be implemented easily in a programming language by means of an if-statement. However, this method slows down any numerical solvers that depend on the NBA-concentration: the sudden jump from under- to oversaturated slows gradient-based search methods down by a lot. The issue is clarified in Fig. 2. The solution is to approximate the concentration of NBA in water using an error function. This has the same slope at low concentrations as the exact solution and the same value at high concentrations, but is smooth and continuous

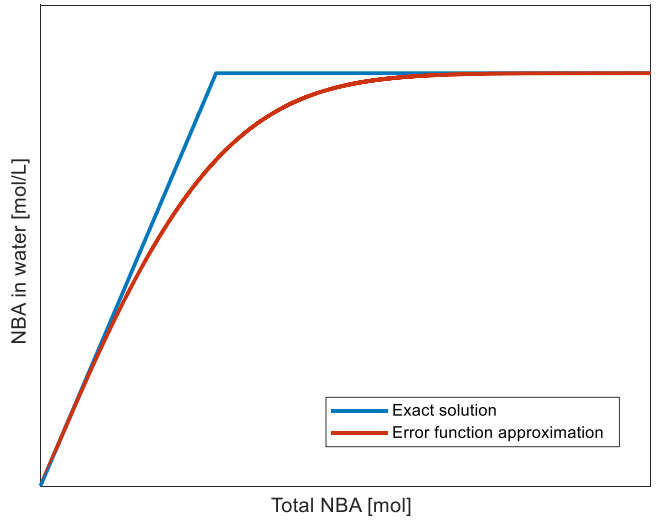

Fig. 2. Concentration of NBA in water in under- and oversaturated systems. Blue denotes exact solution, red an approximation with use of the error function.

over the entire domain:

$$c_{NBA}^{aq} = c_{NBA}^{aq,sat}(T)erf\left(\frac{\sqrt{\pi}}{2}\frac{n_{NBA}}{n_{NBA}^{sat}(T)}\right) \tag{10}$$

For plotting the reaction progress, it is convenient to express the amount of solid NBA as a concentration. The convention used in this work is to determine this concentration on basis of the entire volume of the system:

$$c_{NBA}^{solid} = \frac{n_{NBA}^{solid}}{V^{aq} + V^{org}} \tag{11}$$

2.10. Kinetic model

To describe the rate and final equilibrium of the esterification of xylose with NBA and the extraction of the product to Dowtherm A, a kinetic model was made, shown in Fig. 3. This model incorporates four elementary reaction steps. It should be noted that any water produced in the esterification is not show in the figure, as water is also present as a solvent. The steps can be described as:

1. In the aqueous phase, xylose and NBA form a monoester (NBAX).
2. The monoester partitions over both phases.
3. The monoester reacts with an additional molecule of NBA to form the product ($[NBA]_2X$).
4. NBA is also partitioned over both phases.

This model was formulated to consider several observations in this and previous work [8]:

- There is a final equilibrium between xylose and $[NBA]_2X$.
- Changing the stirring speed does not change the reaction rate.
- Analysis does not reveal any NBAX, and by taking only xylose and $[NBA]_2X$ the mole balance always closes to within 5 %.
- Xylose is only detected in the aqueous phase, and $[NBA]_2X$ in the organic phase.
- When adding NBA stoichiometrically to the mixture, solid NBA is observed at equilibrium op to 60 °C.
- Below 60 °C, the equilibrium concentration of $[NBA]_2X$ with respect to xylose increases at higher temperature, but above 60 °C it decreases.

On the basis of these observations, it can be concluded that:

- All four elementary steps are reversible.
- The rate-determining step does not take place in the boundary layer.
- The system is not limited by mass-transfer.
- Step 1 is rate determining in both ways.
- Steps 1 and 3 have their equilibrium away from NBAX.

This allowed for the following equations to be formulated:

$$K_1 = \frac{c_{[NBA]X}^{aq}}{c_X^{aq} c_{NBA}^{aq}} \tag{12}$$

$$K_2 = \frac{c_{[NBA]X}^{org}}{c_{[NBA]X}^{aq}} \tag{13}$$

$$K_3 = \frac{c_{[NBA]_2X}^{org}}{c_{[NBA]X}^{org} c_{NBA}^{org}} \tag{14}$$

$$K_4 = \frac{c_{NBA}^{org}}{c_{NBA}^{aq}} \tag{15}$$

$$R_e = k_{1e} c_X^{aq} c_{NBA}^{aq} \tag{16}$$

$$R_h = k_{1h} c_{[NBA]X}^{aq} \tag{17}$$

Here, R denotes the reaction rate with subscripts e and h for esterification and hydrolysis respectively. Eqs. (12)–(14) can be multiplied to produce an overall equilibrium constant:

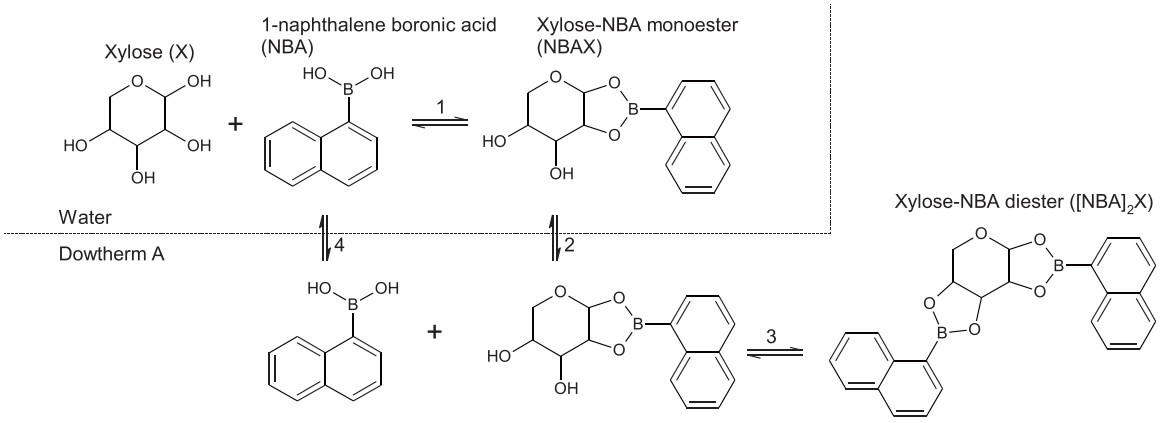

Fig. 3. Kinetic model for the esterification of xylose with NBA and the extraction of the product to Dowtherm A.

$$K_1K_2K_3 = \frac{c^{org}_{[NBA]_2X}}{c^{aq}_X c^{aq}_{NBA} c^{org}_{NBA}} \tag{18}$$

Furthermore, using Eqs. (12), (13), (14) and (18), the hydrolysis rate can be expressed as:

$$R_h = \frac{k_{1e}}{K_1K_2K_3} \frac{c^{org}_{[NBA]_2X}}{c^{org}_{NBA}} \tag{19}$$

The overall observed reaction rate then becomes:

$$R_{obs} = k_{1e}\left(c^{aq}_X c^{aq}_{NBA} - \frac{1}{K_1K_2K_3} \frac{c^{org}_{[NBA]_2X}}{c^{org}_{NBA}}\right) \tag{20}$$

This derivation can be found in more detail in the supplementary information.

With this rate equation, a kinetic model for a batch reaction could be made:

$$\frac{\partial n_X}{\partial t} = -R_{obs}V_{aq} \tag{21}$$

$$\frac{\partial n_{NBA}}{\partial t} = -2R_{obs}V_{aq} \tag{22}$$

$$\frac{\partial n_{[NBA]_2X}}{\partial t} = R_{obs}V_{aq} \tag{23}$$

The concentrations of NBA in the aqueous and organic phase could be derived from the total amount of NBA via these equations:

$$c^{aq,out}_{NBA} = c^{aq,sat}_{NBA}(T) erf\left(\frac{\sqrt{\pi}}{2} \frac{n_{NBA}}{n^{sat}_{NBA}(T)}\right) \tag{24}$$

$$c^{org,out}_{NBA} = K_4 c^{aq,out}_{NBA} \tag{25}$$

Furthermore, it is assumed that xylose and $[NBA]_2X$ only exist in respectively the aqueous and organic phase:

$$c^{aq}_X = \frac{n_X}{V_{aq}} \tag{26}$$

$$c^{org}_{[NBA]_2X} = \frac{n_{[NBA]_2X}}{V_{org}} \tag{27}$$

2.11. CSTR model

Using the previously described model for a batch reactor, a model for a continuous stirred tank reactor (CSTR) was made. Key assumption in this model is that the reactor contents are ideally mixed, which conveniently means that the outgoing concentration is equal to the concentration inside the reactor. Furthermore, all flows (i.e., aqueous, organic and solid) are assumed to have the same residence time. This is defined by:

$$\tau = \frac{V}{\varphi^{org}_v + \varphi^{aq}_v} \tag{28}$$

This allows for defining the aqueous and organic phase volume inside the reactor:

$$V_{aq} = \frac{\varphi^{aq}_v}{\tau} \tag{29}$$

$$V_{org} = \frac{\varphi^{org}_v}{\tau} \tag{30}$$

The residence time is also used to link the flow of solid NBA out of the reactor ($F^{s,out}_{NBA}$) to the amount of solid NBA inside the reactor (n^s_{NBA}):

$$F^{s,out}_{NBA} = \frac{n^s_{NBA}}{\tau} \tag{31}$$

$$\frac{\partial n_{NBA}}{\partial t} = F^{s,in}_{NBA} - F^{s,out}_{NBA} + \varphi^{aq}_v\left(c^{aq,in}_{NBA} - c^{aq,out}_{NBA}\right) + \varphi^{org}_v\left(c^{org,in}_{NBA} - c^{org,out}_{NBA}\right) - 2R_{obs}V_{aq} \tag{32}$$

$$\frac{\partial n_X}{\partial t} = \varphi^{aq}_v\left(c^{in}_X - c_X\right) - R_{obs}V_{aq} \tag{33}$$

$$\frac{\partial n_{[NBA]_2X}}{\partial t} = \varphi^{org}_v\left(c^{in}_{(NBA)_2X} - c^{out}_{(NBA)_2X}\right) + R_{obs}V_{aq} \tag{34}$$

Note that for no flowrate (i.e., infinite residence time) the model simplifies to the batch case.

3. Results and discussion

First, the solubility of NBA was measured, as well as the distribution of NBA in a water-Dowtherm A system. This was measured over a range of temperatures, allowing for the prediction of the NBA concentration in either the aqueous or organic phase if the total amount of NBA and volume of both phases is known. This was needed for further experiments, where the rate and equilibrium of the xylose extraction with NBA are determined in batch experiments. NBA concentrations play a vital role in both the equilibrium and reaction rate. The obtained results are then compared to literature for validation. The validated results of the batch experiments are then used to predict the conversion in a CSTR, which is also experimentally verified. Lastly, the model, based on experimental batch observations and validated with continuous experiments, is used to model a continuous counter-current mixer-settler cascade for the extraction of xylose from a mixture representative of a real biomass feed. This feed is also used to validate a few of the batch experiments.

3.1. NBA solubility and partitioning

The solubility of NBA in water was measured over the temperature range of 5–90 °C using the method described in equipment and procedure. The results are presented in Fig. 4, and the fitted values in Table 1, which can predict the solubility using Eq. (3). The solubility ranges from 0.15 at 5 °C to 5 g/L at 90 °C.

Of note is the obtained value of the melting point, which is much higher than reported in literature (200 – 220 °C) [15]. This is because Eq. (3), to which the data is fitted, is derived for ideal solutions, which is not the case for this solution. For an aromatic molecule like NBA in water, the activity coefficient can be very high. If we take this into account in Eq. (3), the real melting point is probably much lower than

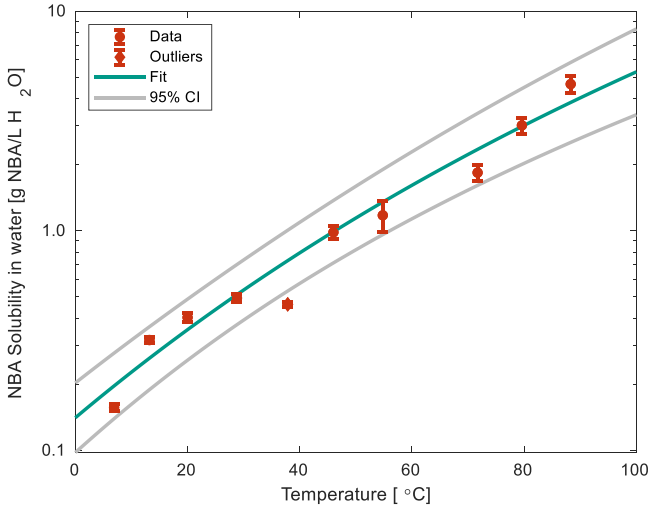

Fig. 4. Solubility of NBA in deionized water in the range of 5–90 °C.

Table 1
Fitted values for Eq. (3) for solubility of NBA in water. Valid from 5–90 °C.

Symbol	Value	95 % confidence bounds		Unit
T_m	1535	1406	1664	K
ΔH_m	31	26	35	kJ/mol

1535 K. This explains why the melting point obtained by fitting is much higher than expected for an organic molecule the size of NBA.

To further investigate this deviation from literature, a TGA-DSC measurement of NBA was done. Fig. 5 shows the DSC and TGA results. The DSC signal clearly shows a peak around the predicted melting point. However, it also shows that a phase transition occurs around 100 °C, paired with significant mass loss that corresponds to 1 mol of water per mole of NBA. This either means that exactly 1 mol of water was present per molecule of NBA as moisture attracted from the air, or that NBA underwent a trimerization to a cyclic boroxine compound, $[NBA]_3$ during the TGA-DSC measurement. The latter was confirmed by FTIR: after TGA-DSC, the sample showed a spectrum that matched that of a known $[NBA]_3$ spectrum [10]. The spectra can be found in the supplementary info. This observation means that when previous literature discusses the melting point of NBA, it is in fact the melting point of $[NBA]_3$. The actual melting point of NBA is much higher than what is previously mentioned, as demonstrated by the solubility experiments.

The partition coefficient (K_4) of NBA in a water/Dowtherm A system was then determined in the temperature range of 20–90 °C as described in equipment and procedure. The results are presented in Fig. 6 and the values as fitted to Eq. (15) in Table 2. The value of K_4 roughly doubles over the range of measurements, from 3.1 at 20 °C to 6.4 at 90 °C.

3.2. Reaction kinetics and equilibria

The reaction rate and final equilibrium for the esterification and extraction of xylose with NBA to Dowtherm A was measured in the temperature range of 20–85 °C using the method described in equipment and procedure. The same experiments were used for fitting the kinetic and equilibrium constants: initial datapoints would give valuable information on the rate, while the last datapoint denoted the equilibrium concentration. The Arrhenius and Van 't Hoff plots are shown in Fig. 7 and Fig. 8, while the fitted values for Eqs. (16) and (18) are listed in Table 3.

Of interest are the large error margins in Fig. 8. These are reflecting the large uncertainty in the measured value of $K_1K_2K_3$, as this depends on the uncertainty in the xylose, $[NBA]_2X$ and NBA concentrations in the

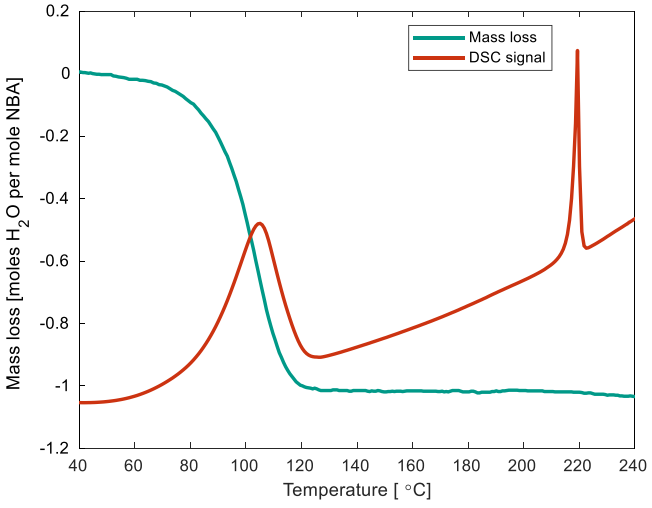

Fig. 5. TGA-DSC analysis of NBA. Protocol used is listed in equipment and procedure.

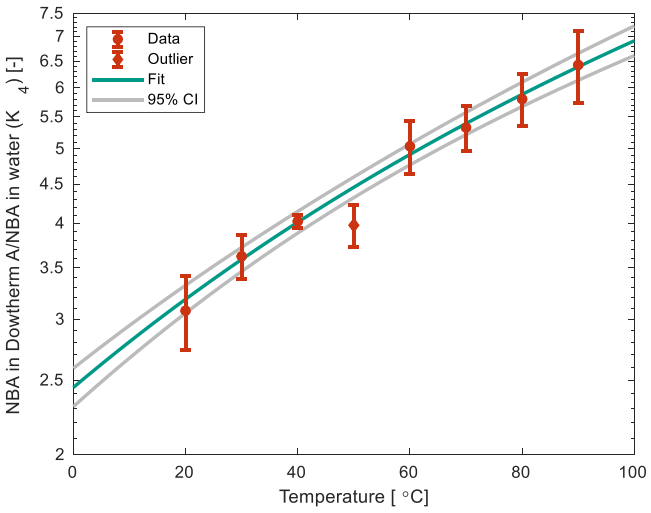

Fig. 6. Partitioning coefficient of NBA in a water/Dowtherm A system between 20 and 90 °C.

Table 2
Fitted values for Eq. (15) of NBA partitioning in a water/Dowtherm A system between 20 and 90 °C.

Symbol	Value	95 % confidence bounds		Unit
ΔS_0	40	38	42	J/mol/K
ΔH_0	8.8	8.1	9.5	kJ/mol

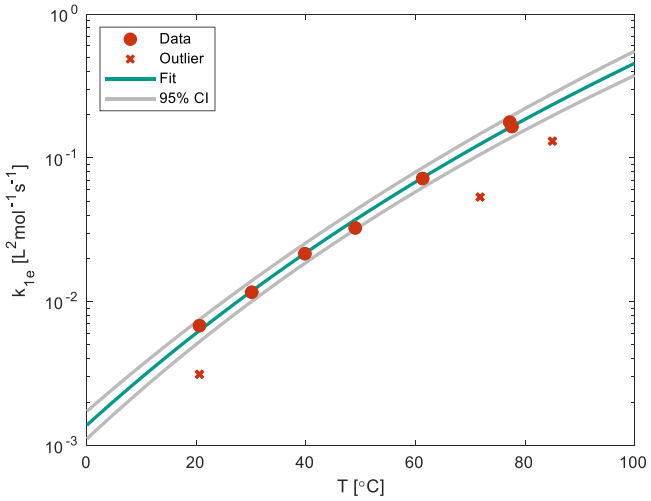

Fig. 7. Arrhenius plot for the esterification of xylose with NBA in a water/Dowtherm A system. Measured between 20 and 85 °C.

aqueous and organic phase. Since they are measured directly, the uncertainties for xylose and $[NBA]_2X$ are small (around 0.5 and 2 % respectively). However, the NBA concentration could not be measured in either phase, and was therefore derived with a mole balance. This balance used the amount of xylose and $[NBA]_2X$ present, as well as the solubility and partition coefficient of NBA, with all their respective uncertainties. This caused a large uncertainty in the NBA concentrations, as evident in Fig. 9, which then caused a large uncertainty in $K_1K_2K_3$.

To validate the model with the fitted values, the model was compared with concentrations over time as obtained for each batch experiment. The same experiments that were used for fitting the kinetic and equilibrium constants were used for this. The model was run by using the values of k_{1e} and $K_1K_2K_3$ as obtained from the fits, i.e., not

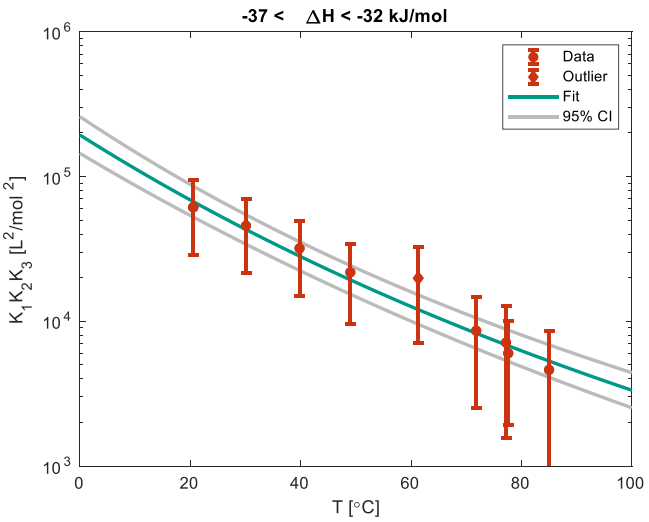

Fig. 8. Van 't Hoff plot for the esterification of xylose with NBA in a water/Dowtherm A system. Measured between 20 and 85 °C.

Table 3
Fitted values for kinetics and equilibrium of esterification of xylose with NBA in a water/Dowtherm A system. Measured between 20 and 85 °C, based on Eqs. (16) and (18).

	Symbol	*Value*	*95 % confidence bounds*		*Unit*
k_{1e}	k_0	15	14	16	L/mol/s
k_{1e}	E_{act}	49	47	52	kJ/mol
$K_1K_2K_3$	ΔS_0	−25	−34	−16	J/mol/K
$K_1K_2K_3$	ΔH_0	−34	−37	−32	kJ/mol

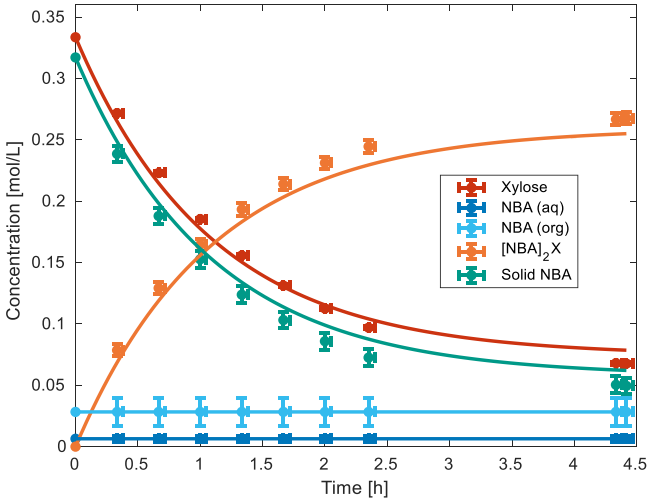

Fig. 9. Experimental and modelled concentrations over time for the extraction of xylose to Dowtherm A via the esterification with NBA. Experiment performed at 49 °C, 1:1 S:F and 3500 W/m^3 stirring input.

from the kinetic and equilibrium constants this one experiment provided. Fig. 9 shows the data for an experiment at 49 °C, which is representative of all other experiments. Data for the other experiments can be found in the Supplementary Information. The figure shows that the model is a good fit for the experiment it was based on.

To further validate the model, it was compared to older own data that we published in literature [8]. Our earlier publications reported a quadratic increase in $[NBA]_2X$ concentration with increasing xylose concentration but could not propose a theoretical explanation for this.

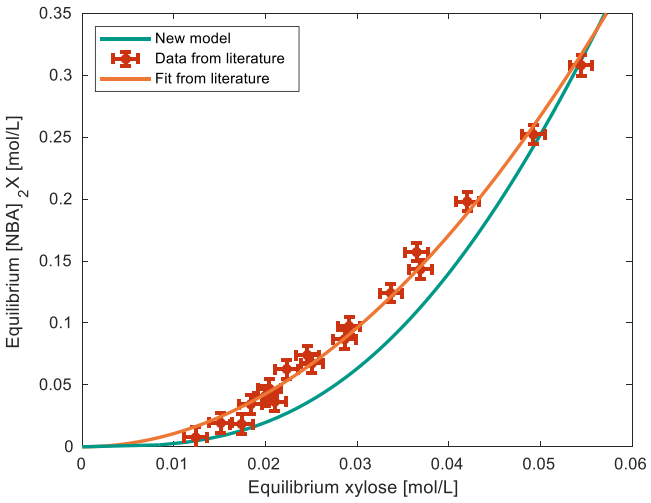

Fig. 10. Equilibrium curve for the xylose/NBA/water/Dowtherm A system. S:F of 1:1, temperature of 85 °C and 2 moles NBA per mole of xylose. Literature data from [8].

Fig. 10 shows the equilibrium data from literature, together with the old quadratic fit and the predication by the new model. The model slightly underpredicts the $[NBA]_2X$ concentration at equilibrium but is overall in good agreement with previous observations.

Moreover, the impact of the ratio of NBA to xylose on the NBA conversions was slightly better described with our new model as shown in Fig. 11. Overall, it can be concluded that the new model does not only accurately predict the findings of this publication, but also the results of other publications.

While Fig. 8 shows that the esterification of xylose with NBA is an exothermic reaction, it was observed in practice that the extraction yield was increased with temperature. With the help of the model, this can be understood, if we make some modifications. The reason for this behavior is that at lower temperatures, the extraction yield at equilibrium is not determined by the amount of chemicals present, but more by the solubility of NBA. On the other hand, at higher temperatures, the system behaves 'normally', i.e. the solubility of NBA is higher that the concentration at equilibrium. Fig. 12 shows this: here, the model is run normally, once without taking the solubility into account (i.e. the NBA concentration can be higher than the solubility), and once where the

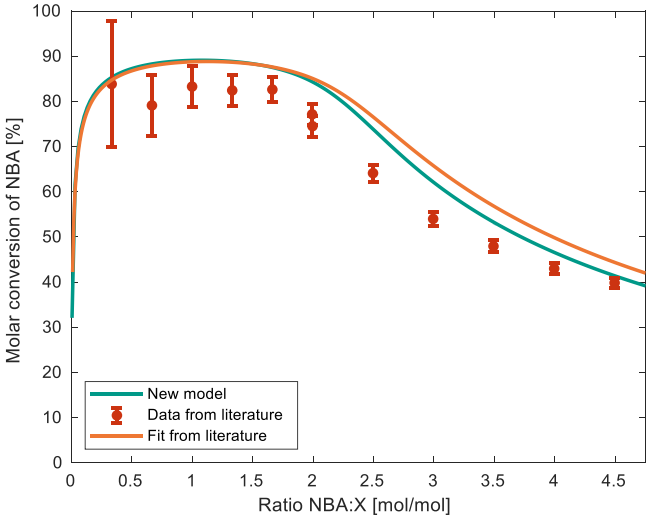

Fig. 11. Equilibrium conversion of NBA for the xylose/NBA/water/Dowtherm A system. S:F of 1:1, temperature of 85 °C and initial concentration of xylose of 0.33 mol/L. Literature data from [8].

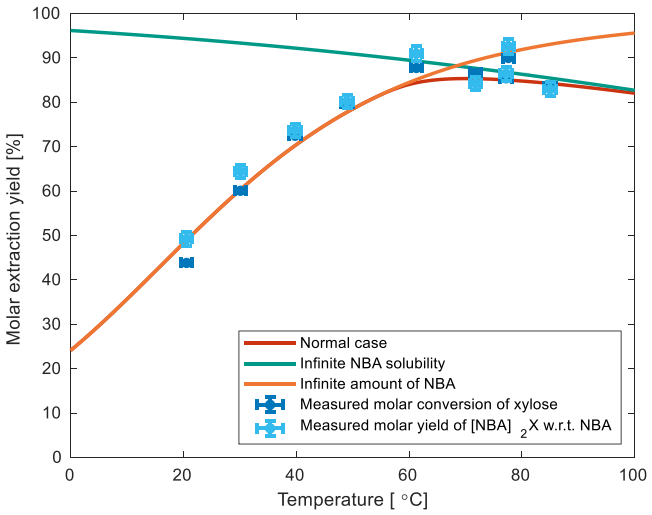

Fig. 12. Equilibrium extraction yield of xylose to Dowtherm A via esterification with NBA. S:F of 1:1, initial xylose 0.33 mol/L and 2 moles NBA per mole xylose.

NBA concentration is always at solubility (i.e. there is an infinite amount of NBA). The same datapoints which made up Fig. 7 and Fig. 8 are also plotted.

The figure clearly shows that at lower temperatures, the system behaves as if there is an infinite amount of NBA, as the equilibrium is limited by the solubility of NBA. At 60 – 80 °C there is a transition region, and above 80 °C, the solubility of NBA no longer limited the equilibrium. Interestingly, this figure also explains the outlier in Fig. 8 at 60 °C: the system behaved as if it was already in the region where solubility is no longer an issue, even though theory predicted solubility to still be an issue. The same can be said for the datapoints at 80 °C, where one datapoint behaves as if not all NBA is dissolved, while it should be the case. The graphs also indicate an optimum in the equilibrium yield at 70 °C of 85 % moles of xylose extracted. After this, the equilibrium drops slightly to 82 % at 100 °C.

Another observation made during these batch extraction experiments is that the water/Dowtherm A mixture can be difficult to separate into two phases. Normally, they do so quite readily, but when NBA is added for the extraction, the emulsions formed in the extraction never phase-separated spontaneously, but always needed centrifugation, as also stated in Equipment and Procedure. This is the case for all samples drawn during the batch experiments. The final mixture inside the reactor, still at reaction temperature, also hardly phase separated on its own. There is one exception though: at high temperatures, and at the end of the extraction, the mixture inside the reactor did separate into two phases. This was from 70 °C and higher, corresponding to the region in Fig. 12 where NBA is fully dissolved at equilibrium. These observations could be explained by an emulsifier-like behavior of solid NBA, helping stabilize the solution when it is present as a solid.

3.3. CSTR experiments

Having extensively measured the batch system, it was possible to create a model for the continuous extraction of xylose to Dowtherm A via esterification with NBA. This model is based on Eqs. (32)–(34), and experimentally verified.

The experimental setup is described in equipment and procedure. All experiments used a 0.33 mol/L (5.0 wt%) solution of xylose in water and 0.66 mol/L (11.5 wt%) suspension of NBA in Dowtherm A as starting material. These were pumped through the reactor at various pump speeds, thereby changing the residence time inside the vessel. Note that both phases were pumped by two pumps on one axle, meaning that the ratio between the two were always the same. Since the starting materials were colder than the heated jacket of the reactor, changing the pump speed also influenced the temperature inside the reactor, which varied from 73 to 93 °C for these experiments. The conversion of xylose and NBA were measured, as was the yield of $[NBA]_2X$ for these experiments. Fig. 13 shows the result of these experiments and compares them to the prediction made by the CSTR model, as described previously.

Fig. 13 shows that for longer residence times, more xylose is extracted. Around 5 minutes, half of the initial amount is extracted, and equilibrium at 100 minutes. This is to be expected, as the esterification reaction with NBA is not instantaneous. The model does underpredict the extent of extraction for most datapoints. This could be attributed to several reasons. First of all, the model assumes a perfect CSTR with its residence time distribution (RTD). In reality, the reactor probably exhibits the RTD of a few CSTRs in series, which improves xylose conversion. Furthermore, the liquids are mixed before entering the reactor, and do not instantly phase separate after leaving the reactor. This could lead to extraction occurring before and after the reactor, also improving yield.

Fig. 14 shows the dependency on the amount of stirring of the amount of xylose extracted as $[NBA]_2X$ to Dowtherm A at equal residence times and temperatures in the continuous extraction setup. It is clear that stirring has a large influence, as over the entire range of measured power inputs, the yield increases. This indicates that mass transfer can play a role at elevated temperatures, and that good stirring is vital to a high single-pass yield of the extraction. A simple extraction column would therefore not suffice, but a mixer-settler cascade would be more appropriate.

3.4. CSTR cascade modelling

Having established the model for CSTR extraction of xylose, it was used to design a continuous countercurrent cascade for this extraction. The model is a simple mixer-settler cascade, as described in Eqs. (32)–(34). The aqueous phase flows counter-currently to the organic phase, and any solid NBA flows with the organic phase. This choice was made as in the experiments with the CSTR, the reactor effluent always had to be centrifuged. This left the NBA and Dowtherm A on the bottom of the centrifuge tube, and water on top. In the model, all phase separations are assumed to be complete.

The design specification of the cascade is to extract 90 % of the xylose in a 5 wt% (0.33 mol/L) feed stream. The cascade will be operated at 90 °C, as kinetics are most favorable, equilibrium does not suffer,

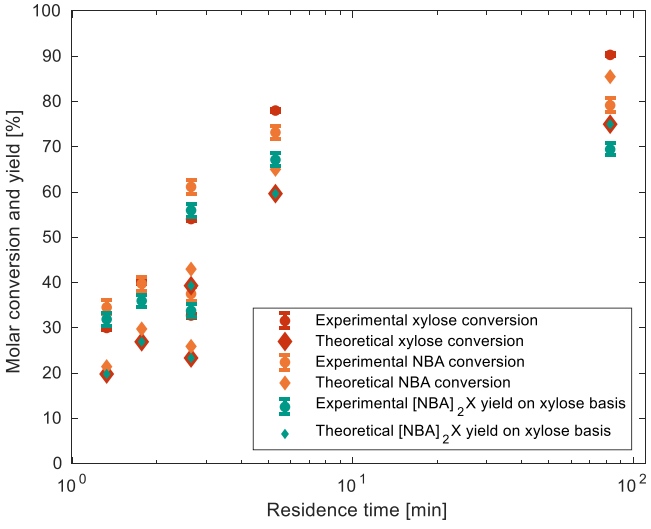

Fig. 13. Experimental and theoretical conversion and yield for extraction of xylose from water to Dowtherm A via esterification with NBA. S:F of 1:0.93, initial xylose 0.33 mol/L in water (F) and 0.66 mol/l NBA in Dowtherm A (S).

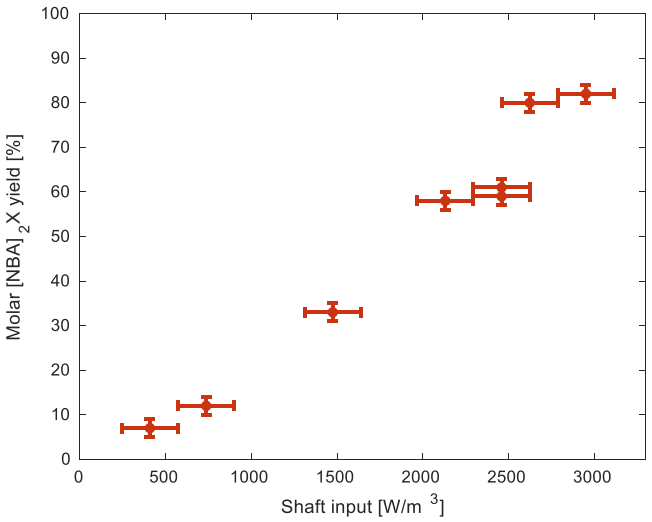

Fig. 14. $[NBA]_2X$ in a continuous extraction setup for various stirrer shaft power input. All extractions were carried out in a 1:1 S:F system, with 0.33 mol/L initial xylose in water and 2 moles of NBA per mole of xylose fed as a suspension in Dowtherm A. The temperature was 85 °C for all experiments, and 0.1 mL/s of each liquid.

and the feed streams do not need to be cooled down as much, while still allowing for operation at atmospheric pressure. NBA will be fed 2.2 moles per mole of xylose, as more does not improve extraction, but less is very detrimental to the amount of sugars extracted. The cascade will be operated at a volumetric solvent-to-feed ratio (S:F) of 1:1; while lower S:F would make the cascade smaller and concentrate the $[NBA]_2X$ solution, the solubility of $[NBA]_2X$ is around 0.33 mol/L at room temperature, making handling and analysis of solutions with higher concentrations difficult.

The model was run for various amounts of stages and residence time, in order to obtain the smallest amount of stages and total volume. The residence time on each stage was equal, and the total residence time was the same regardless of the total amount of stages. This means that in Fig. 14, where the results are plotted, a cascade with a residence time of 10 minutes with 2 stages has a residence time of 5 minutes per stages, but one with 24 stages, 25 second residence time per stage.

Fig. 14 shows that at least two stages are needed for a 90 % recovery of xylose with a total residence time of 8 minutes. Three would make the cascade significantly smaller (by a factor 2), but any additional stages would have little effect. For the three-stage cascade, a total residence time of 4 minutes is needed. This means that 0.36 ton sugar per m^3 cascade per hour is extracted. This is above the threshold of 0.1 $t/m^3/h$, which other research uses as a benchmark for being industrially applicable [16].

One note with this cascade is that a significant part of the boronic acid is not converted to $[NBA]_2X$. Since 90 % of the xylose is extracted on a molar basis, and NBA is fed 2.2:1 on molar basis, 18 % of the fed NBA is not converted. As indicated by Fig. 12, at this temperature, no solid NBA is left after the extraction. Any unconverted boronic ester is therefore dissolved in the aqueous or organic phase. Any in the organic phase is not lost, as that phase is continuously recycled throughout the process (Fig. 1). However, NBA in the aqueous phase may be lost if the aqueous phase cannot be re-used for hydrolysis. At the suggested conditions for extracting 90 % of the xylose, 3.2 % of the NBA fed to the cascade will end up dissolved in the aqueous phase. Of this, 86.6 % can be recovered as a solid when the liquid is cooled down to 30 °C.

3.5. Hydrolysate experiments

To verify that the findings of this study are also applicable to a real feedstock, i.e. from biomass, experiments were conducted with acid hydrolysate of bagasse (ABH), as described in equipment and procedure. The main points of focus were:

- How much of each type of sugar present in ABH is extracted via esterification with NBA to Dowtherm A at the proposed process conditions?
- How many contaminants are co-extracted with the sugars at these conditions?
- Once the sugars have been extracted, can the raffinate be re-used in the hydrolysis?

The ABH was prepared as previously described, and then contacted with Dowtherm A at 90 °C in a shake bath for 24 hours, similarly to how the partition of NBA was determined in a water-Dowtherm A system. This was done once without NBA and with NBA: the experiment without NBA served to quantify the amount of contaminants (i.e. everything except the carbohydrates) extracted, and the one with NBA for the amount of sugars extracted.

Table 4 lists how much of each component was present in the ABH before the extraction, and how much of each was extracted. No significant change indicates that the 95 % confidence interval of the amount extracted includes zero. The amount of xylose extracted is in-line with the findings earlier in this work (Fig. 12). The amount of other sugars is mostly comparable to prior work ([7]) with the clear exception of arabinose. Previously, around 5 % of arabinose was extracted via esterification with a boronic acid, while this work shows a 13-fold increase. However, in the prior work referenced, the extraction was done with phenyl boronic acid and toluene at room temperature, all three different from this work. This does not seem to affect extractive yield of the other sugars, though.

Concerning the contaminants, only furfural was significantly extracted. This, however, should not pose a problem for a process where the sugar-boronate esters are converted into furfural, as all furfural is afterwards distilled out of the solvent. 5-HMF was present in such small amounts, that it was impossible to state whether any was extracted. Acetic acid was present in the ABH in large quantities, but none was extracted to the organic phase. If the raffinate of this extraction were to be reused for hydrolysis, the acetic acid would have to be removed, as it would otherwise accumulate. An extraction with ethyl acetate would be an option.

Any polymeric contaminants which could not be detected with HPLC were quantified by MCRT and GPC. MCRT could give a rough estimate of the absolute amount of polymers present in the extract, and GPC on the size of them. MCRT was only done on the organic phase, as the feed was free of any contaminants, and the extract (when extracting without NBA) should only contain contaminants, allowing for easy quantification. This yielded a 56 ppm carbon residue of the Dowtherm A extract after contact with the ABH at 90 °C without NBA for 24 hours. This was close to the detection limit but does show that very little polymers migrate from the aqueous to the organic phase. GPC also underlines this, as no large (> 0.7 kDa) polymers could be detected.

One kind of contaminant which could not be analyzed was a solid layer appearing when ABH and Dowtherm A were mixed. The ABH was filtered, free from any solids, and no NBA was added in this case. Still,

Table 4
Initial concentration and amount extracted of sugars and contaminants in ABH by contacting with Dowtherm A and NBA for 24 hours at 90 °C.

	Initial amount (g/L)	*Extracted (wt%)*
Xylose	29.83 ± 0.70	87.5 ± 2.3
Glucose	1.97 ± 0.11	39.0 ± 6.4
Arabinose	2.43 ± 0.03	67.4 ± 1.1
Galactose	0.26 ± 0.07	No significant change
Furfural	1.87 ± 0.19	81.5 ± 10.3
5-HMF	0.06 ± 0.02	No significant change
Acetic acid	6.34 ± 0.39	No significant change

solids appeared at the interface at room temperature. Fig. 15 is a photo of the appeared solid phase after centrifugation to fully phase separate the three phases. An attempt was made to recover the solids for analysis. This was done by first carefully removing the clean liquid phases, and then dissolving the remaining liquids and solid in acetone. The acetone, water and Dowtherm A were evaporated off, but barely any solid material remained. Analysis of this newly formed solid could therefore not be performed.

The ABH was also titrated with a 0.3 mol/L solution of NaOH in water with thymol blue as indicator. As the titration progressed, the solution turned turbid, which also occurred when samples for HPLC running the Pb-column were neutralized with KOH. It was, however, still possible to see the transition of yellow to blue, indication the end of the titration. The endpoint matched the amount of acid that was expected from the initial 1 wt% H_2SO_4 and the formed acetic acid. This indicates that no sulfuric acid is consumed during the hydrolysis.

While the concentration of H_2SO_4 in the hydrolysate was similar to the initial amount, the total liquid volume was not. It was noted that, not taking into account losses due to handling, 13.0 % of the total liquid was lost in the hydrolysis process per pass. This could be attributed to the solid waste after hydrolysis: not all fibers of the bagasse are broken down, and the solid residue needs to be removed from the liquid by filtration. The resulting filter cake is wet with the hydrolysate, which accounts for all 13.0 % mass loss. For the proposed two-stage extraction, this means that only 75.7 % of the initial liquid is left at the end of the hydrolysis process.

This mass loss has a few implications: first, the extraction is best carried out before the solid residue is filtered from the hydrolysate. Secondly, even if the lean hydrolysate is reused, a significant make-up stream of water and sulfuric acid is needed. The upside is, though, that the lost liquid acts as a purge, preventing the buildup of non-extracted compounds, such as 5-HMF, some sugars, and acetic acid.

4. Conclusion

The solubility of NBA was measured for various temperatures, as well as the partitioning over a water/Dowtherm A system. The extraction rate and equilibrium of xylose from water to Dowtherm A was also measured over a range of temperatures. Together, this data was used to make a kinetic model of the extraction, which took into account the limited solubility of NBA. The model was shown to be a good fit for the measurements of this work and of previous work. The same model was used to predict the extent of extraction for a CSTR, which was experimentally verified. An extraction cascade could then be designed, showing that three units are needed with a total residence time of 11 minutes to extract 90 % of the xylose from an aqueous feed stream. All findings were also validated with ABH, and it was found that after extracting the sugars from the ABH, the raffinate can be reused in the hydrolysis.

CRediT authorship contribution statement

Sascha Kersten: Writing – review & editing, Supervision, Resources, Project administration, Investigation, Funding acquisition. **Jean-Paul Lange:** Writing – review & editing, Supervision, Funding acquisition, Conceptualization. **María Pilar Ruiz:** Writing – review & editing, Supervision, Project administration. **Peter van der Wal:** Writing – original draft, Methodology, Investigation, Formal analysis, Data curation.

Declaration of Competing Interest

The authors declare the following financial interests/personal relationships which may be considered as potential competing interests: Peter van der Wal reports financial support was provided by Shell. If there are other authors, they declare that they have no known competing financial interests or personal relationships that could have appeared to influence the work reported in this paper.

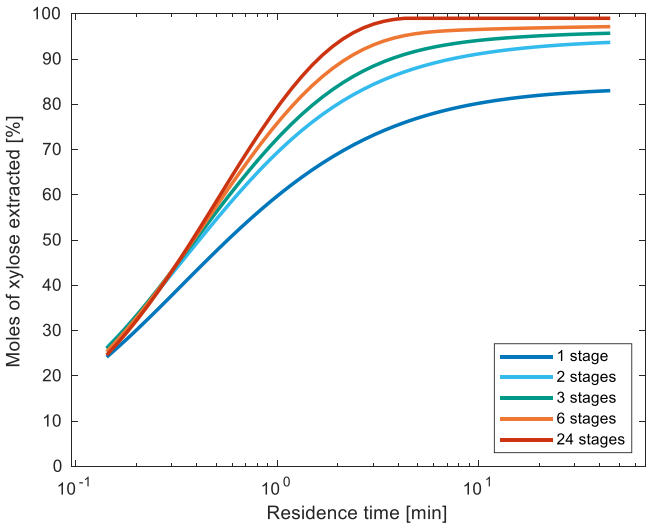

Fig. 15. Modelled extraction yield of xylose to Dowtherm A via esterification with NBA for various residence times and stages in a countercurrent mixer-settler cascade. Conditions: 90°C, 1:1 S:F, 2:1 NBA:xylose, 0.33 mol/L xylose in feed.

Fig. 16. Photo of centrifuge vial (10 mL total volume) containing ABH (top), Dowtherm A (bottom) and the solid phase that appeared on the interface.

Acknowledgments

The authors would like to thank Shell Global Solutions International B.V. for funding this research and Benno Knaken, Ronald Borst, Raymond Spanjer, Johan Achterhorst and Erna Fränzel-Luiten for the technical support and expertise. Furthermore, we would like to Casper van Dongen for his large contribution to the data in Fig. 14.

Appendix A. Supporting information

Supplementary data associated with this article can be found in the online version at doi:10.1016/j.jece.2024.115226.

Data availability

Data will be made available on request.

References

[1] J.P. Lange, "Furfural manufacture and valorization – A selection of recent developments," 2024, Elsevier B.V. doi: 10.1016/j.cattod.2024.114726.

[2] J.P. Lange, E. Van Der Heide, J. Van Buijtenen, and R. Price, "Furfural-A promising platform for lignocellulosic biofuels," 2012, Wiley-VCH Verlag. doi: 10.1002/cssc.201100648.

[3] N. Gathergood, M. Granados, and D.Martin Alonso, Furfural: An Entry Point of Lignocellulose in Biorefineries to Produce Renewable Chemicals, Polymers, and Biofuels. 2018. doi: 10.1142/q0142..

[4] L. Ricciardi, W. Verboom, J.P. Lange, J. Huskens, Kinetic model for the dehydration of xylose to furfural from a boronate diester precursor, RSC Adv. 12 (49) (2022) 31818–31829, https://doi.org/10.1039/d2ra06898b.

[5] L. Ricciardi, W. Verboom, J.P. Lange, J. Huskens, Selectivity switch by phase switch-the key to a high-yield furfural process, Green. Chem. 23 (20) (2021) 8079–8088, https://doi.org/10.1039/d1gc01752g.

[6] L. Ricciardi, W. Verboom, J.P. Lange, J. Huskens, Synergic effects of boronate diester formation and high-ionic strength biphasic operation on xylose-to-furfural selectivity, ACS Sustain Chem. Eng. 10 (11) (2022) 3595–3603, https://doi.org/10.1021/acssuschemeng.1c08265.

[7] L. Ricciardi, W. Verboom, J.P. Lange, J. Huskens, Selective extraction of xylose from acidic hydrolysate-from fundamentals to process, ACS Sustain Chem. Eng. 9 (19) (2021) 6632–6638, https://doi.org/10.1021/acssuschemeng.1c00167.

[8] P.J. van der Wal, S.R.A. Kersten, J.-P. Lange, M.P. Ruiz, Process development on the high-yielding reactive extraction of xylose with boronic acids, Ind. Eng. Chem. Res 62 (20) (2023) 8002–8009, https://doi.org/10.1021/acs.iecr.3c00364.

[9] G.J. Griffin, L. Shu, Solvent extraction and purification of sugars from hemicellulose hydrolysates using boronic acid carriers, J. Chem. Technol. Biotechnol. 79 (5) (2004) 505–511, https://doi.org/10.1002/jctb.1013.

[10] P.J. van der Wal, J.P. Lange, S.R.A. Kersten, M.P. Ruiz, Kinetics of furfural formation from xylose via a boronic ester intermediate, ACS Sustain Chem. Eng. (2023), https://doi.org/10.1021/acssuschemeng.3c07390.

[11] J.E. de Paiva, I.R. Maldonade, A.R.P. Scamparini, Xylose production from sugarcane bagasse by surface response methodology, Rev. Bras. De. Eng. Agr. ícola e Ambient. 13 (1) (2009) 75–80, https://doi.org/10.1590/S1415-43662009000100011.

[12] M. Neureiter, H. Danner, C. Thomasser, B. Saidi, R. Braun, Dilute-acid hydrolysis of sugarcane bagasse at varying conditions, Appl. Biochem Biotechnol. 98 (1) (2002) 49–58, https://doi.org/10.1385/ABAB:98-100:1-9:49.

[13] M. Schwaab, J.C. Pinto, Optimum reference temperature for reparameterization of the Arrhenius equation. Part 1: Problems involving one kinetic constant, Chem. Eng. Sci. 62 (10) (2007) 2750–2764, https://doi.org/10.1016/j.ces.2007.02.020.

[14] P.W. Atkins, J.De Paula, J. Keeler. Atkins' Physical Chemistry, Twelfth Edition, Oxford University Press, New York, NY, 2023.

[15] K. Kielar, O.M. Demchuk, K.M. Pietrusiewicz, General approach to the synthesis of prochiral atropisomeric biaryls, *ISRN Org. Chem.*, Vol. 2011 (2011) 1–11, https://doi.org/10.5402/2011/919102.

[16] J.P. Lange, Catalysis for biorefineries-performance criteria for industrial operation, R. Soc. Chem. (2016), https://doi.org/10.1039/c6cy00431h.